Received 5 February 2021; revised 9 March 2021; accepted 21 March 2021. Date of publication 29 March 2021; date of current version 9 April 2021.

Digital Object Identifier 10.1109/OJCOMS.2021.3069253

Weighted-Sum-Rate Maximization for an Reconfigurable Intelligent Surface Aided Vehicular Network

DILIN LALINDRA DAMPAHALAGE (Graduate Student Member, IEEE), K. B. SHASHIKA MANOSHA (Member, IEEE), NANDANA RAJATHEVA (Senior Member, IEEE), AND MATTI LATVA-AHO (Senior Member, IEEE)

Centre for Wireless Communications, University of Oulu, 90570 Oulu, Finland

CORRESPONDING AUTHOR: D. L. DAMPAHALAGE (e-mail: dilin.dampahalage@oulu.fi)

This work was supported by the Academy of Finland 6Genesis Flagship under Grant 318927, and in part by Business Finland MOSSAF project.

ABSTRACT Recently, reconfigurable intelligent surfaces (RISs) have been identified as one potential solution to avoid performance degradation of using millimeter wave (mmWave) frequencies in vehicular communications. In this paper, we investigate the use of an RIS in a mmWave vehicular communication network. The problem of weighted sum-rate maximization in the uplink is considered, where an RIS is used to assist the communication. We focus on both single-user and multi-user cases. Single user case is solved using successive refinement algorithm, where two phase-optimization schemes that help reducing the channel estimation overhead are considered. In multi-user case, fractional programming technique is used to reformulate the original problem into a more convenient form, and an algorithm based on alternating optimization is proposed. The validity of the proposed methods is confirmed by numerical simulations. A significant performance increase is seen when utilizing an RIS in both cases. Considered phase optimization schemes are shown to result in a significant reduction in channel estimation at a cost of small performance degradation compared to the full channel state information beamforming scenario. We perform simulations to investigate the effects of mobility, and the results demonstrate the ability of an RIS to mitigate the effects of mobility to some extent. Furthermore, to get practical insights into vehicular communications aided by an RIS, we use a commercial ray-tracing tool to evaluate the performance.

INDEX TERMS Alternating optimization, fractional programming, mmWave communications, passive beamforming, ray tracing, reconfigurable intelligent surfaces, vehicular communications.

I. INTRODUCTION

TODAY we rely heavily on real time information such as traffic conditions, weather changes and updates on road regulations to have a smooth and efficient driving experience. Also, vehicle manufacturers are putting more and more safety mechanisms into vehicles. A vehicle in the future will need to communicate with a lot of devices nearby consisting of other vehicles, roadside sensors and wireless access points, to provide autonomous driving capabilities giving additional safety and comfort for the passengers. All these applications depend on wireless communication to connect to devices with high reliability, low latency, and higher data rates. However, the inherent randomness in the wireless propagation environment brings challenges to the connectivity. Recently, RISs have been introduced into the wireless communication landscape as a means to control the wireless propagation environment with software-controlled reflections [1].

Generally, an RIS consists of large number of passive reflecting elements arranged in a planar array. The phase shift of each of the reflecting elements can be controlled independently in an intelligent manner to improve the communication. Advanced relaying, which was a significant topic some time ago, also controls the signal propagation between endpoints. However, reflecting elements of RIS are passive and they do not have any active transmit radio frequency (RF) chains, making it possible to be implemented with low hardware complexity and operated with low energy costs [2]. Also, RIS can naturally operate in full-duplex (FD) mode

and is free of noise amplification at antennas as well as self-interference [3]. An RIS will be a low-profile auxiliary device that can be easily integrated into an existing communication network transparently, providing great flexibility and compatibility in terms of deployment [3].

The information transfer capabilities of RISs are analyzed in [4] and it is established that the normalized capacity is linearly proportional to the average transmitted energy per square meter, which is an improvement over massive multiple-input multiple-output (MIMO) systems. The existing communication in the wireless network can be improved by using an RIS. For example, the received signal power at the user can be increased by controlling RIS phase shifts with the reflected signal being added constructively. The interference can be reduced by controlling RIS phase shifts with the reflected signal being added destructively. When utilizing an RIS we need to optimize the phase shifts at the RIS in addition to transmit/receive beamforming. This is known as passive beamforming or phase optimization. The problem of solving joint transmit beamforming and passive beamforming is considered in [5]. They propose an efficient algorithm based on the alternating optimization of phase shifts and transmit beamforming vector in an iterative manner. In [6], this is further extended to consider discrete phase shifts at the RIS, which is an important consideration since practical implementation is possible with only discrete phase shifts.

The effective channel through RIS consists of three components, namely, the direct channel from BS to the user, indirect channel from BS to RIS and reflection channel from RIS to user. A reflecting element in the RIS captures the transmitted signal and re-scatters it in every direction [7], [8]. As a result of the scattering nature of RIS elements, the total path loss through RIS is the product of the path losses through transmitter to RIS and RIS to receiver links [8]. A large number of reflecting elements are needed to compensate for this severe path loss by means of passive beamforming. Furthermore, the careful positioning of the RIS is important in order to get the full benefits of RIS as pointed out by the simulations in [7].

Passive beamforming depends on accurate channel estimates being available. However, estimating the channel at the RIS is difficult since the reconfigurable surface consists of passive elements and limited processing power is available at the RIS. In [9], a scheme that divides RIS elements into groups which shares a common reflection coefficient has been considered. This reduces the channel estimation overhead, since only the combined channel of each group needs to be estimated. In [10], a scheme that only leverages the angle of arrival (AoA) of the line-of-sight (LoS) BS-RIS channel and the angle of departure (AoD) of the LoS RIS-User channel to design the reflecting matrix has been utilized, to reduce computational complexity of RIS reflection matrix. Two schemes that can be used for RIS channel estimation are proposed in [11]. In their work they consider an RIS having few active elements in addition to the passive elements. These active elements can be used to take measurements of the channel. The first method uses compressive sensing to construct the complete channel state information (CSI) from the sparse measurements taken. In the second method, a deep learning model is trained to interact with the incident signal, given the channel measured by the active elements.

However, most theoretical work assumes full CSI being available at the BS, which will be hard to obtain in practice as pointed out earlier. Therefore, it is important to investigate robust transmission strategies for RIS aided communications. Robust active precoder and passive reflection beamforming design is investigated in [12] based on the assumption of an imperfect reflection channel. The reflection channel uncertainties are addressed using an ellipsoid model. They consider the transmit power minimization problem at the BS by jointly designing active precoder at the BS and passive beamforming at RIS while ensuring the quality of service (QoS) requirements of all users are met under all channel error realizations. Robust transmission design based on imperfect cascaded BS-RIS-user channels is presented in [13]. They consider the design of a robust active and passive beamforming scheme to minimize the total transmit power under both the bounded CSI error model and statistical CSI error model.

Vehicular communications have been heavily studied in literature to realize the concept of intelligent transportation systems (ITS) [14]. There are various vehicular applications emerged including safety related, passenger comfort and entertainment applications. Autonomous driving vehicles are also being heavily focused and invested [15], and they will soon be ready for everyday use. However, they bring great challenges in terms of wireless communications. The reason is they consist of various data intensive sensors such as light detection and ranging (LiDAR) sensors, radio detection and ranging (RADAR) sensors and cameras [16]. Intel has estimated that on average an autonomous vehicle will generate about 4TB of data per day, with LiDARs and cameras generating between 10-70 MB and 20-40 MB per second respectively [17]. Traditionally, dedicated short-range communication (DSRC) standard has been used to support vehicular communications. It can support data rates up to 27 Mb/s within a 1 Km radius. However, recent usage of data intensive sensors has resulted in vehicular communication networks having to support Gb/s data rates [14]. These high data rates require a large system bandwidth which can be hardly supported by existing sub-6 GHz cellular networks. These facts have motivated the utilization of mmWave frequency band (10 GHz-300 GHz) that has a largely available bandwidth [14] for vehicular communications. However, mmWave frequencies experience a higher path loss, thus reducing the transmission range. Large antenna arrays that can achieve a significant beamforming gain, are needed in order to compensate for this severe path loss [18]. On the other hand, the high directivity in mmWave communication make it vulnerable to blockages,

which will be frequent in urban environments where vehicles will be driven normally. Recently, RISs have been proposed in [19] to overcome these challenges. They consider a scenario where multiple RISs are deployed to assist downlink mmWave communication. The received power is maximized by jointly optimizing transmit beamforming at the BS and passive beamforming at the RIS.

RIS assisted vehicular communication has recently gained some attention in the literature. In [20], an RIS enabled vehicular network is investigated to improve the physical layer security. They have presented two vehicular network models, one with an RIS based access point (AP) and another model with an RIS based relay. The outage probability of an RIS assisted vehicular networks is analyzed in [21]. They have compared the outage performance of traditional vehicular networks and RIS aided vehicular networks. Resource allocation for an RIS assisted vehicular communications is studied in [22], where vehicle-to-vehicle (V2V) and vehicle-to-infrastructure (V2I) links with different QoS requirements share spectrum. They consider the sum V2I capacity maximization problem while guaranteeing the signal-to-interference-plus-noise ratio (SINR) of the V2V links. This is associated with the joint optimization of power coefficients, RIS reflection coefficients and spectrum allocation.

To the best of authors' knowledge, the RIS aided weighted sum rate (WSR) maximization problem for mmWave vehicular uplink is not investigated in the literature. Although, WSR maximization for RIS aided communication systems are investigated in [23], [24] and [25], those did not consider the vehicular scenario, and a continuous phase shift model is used for the RIS. WSR maximization for an RIS aided multiple-input single-output (MISO) downlink communication system is investigated in [25], where the authors use fractional programming (FP) techniques [26] to decompose the original problem into four disjoint blocks and to design a low-complexity algorithm based on the non-convex block coordinate descent (BCD) method. The achievable rate maximization in uplink of a mmWave vehicular communication network is investigated in the conference article [27], which we extend to consider multiple vehicles with the current work.

In this paper, we consider the uplink of a mmWave vehicular network. Specifically, we model the network with a single BS having multiple antennas and multiple vehicles each with a single antenna. We introduce an RIS to improve the uplink communication between the vehicles and the BS. We consider discrete phase shifts at the RIS to closely resemble the practical implementation, and we focus on the problem of WSR maximization and provide solutions for single user and multi-user cases separately. The main contributions of this paper are summarized as follows:

1) For the single-user case, we focus on the phase optimization problem at the RIS. The proposed algorithm is based on successive refinement, and it has much lower complexity than an exhaustive search. In addition, we also consider two other schemes for RIS phase optimization. One method is based on grouping reflecting elements in a large RIS, and the other one is based on position-based passive beamforming. Both these methods help to reduce the channel estimation overhead, and we evaluate the applicability of these two methods in the mmWave vehicular network considered.
2) For the multi-user case, we reformulate the original problem to a convenient form by using FP, and then the proposed solution approach is based on alternating optimization.
3) We perform simulations focusing on the time varying channel of a moving vehicle, to better understand the impact of an RIS in a vehicular network.

The numerical results show that the performance can be significantly improved by utilizing an RIS in both single-user and multi-user cases. The considered phase optimization scheme with grouping provides a significant reduction in the number of channel paths to be estimated while having only a small performance degradation compared to full CSI. Position based passive beamforming is also shown to be useful in reducing the channel estimation overhead while reaching the performance of full CSI for a large reflecting array of 256 elements. For the multi-user case, it is observed that the RIS can facilitate a user in close vicinity to communicate with a high rate. The numerical results also show that the effects of the mobility can be mitigated to an extent through the use of an RIS, which enables its usage in a vehicular network. Furthermore, to gain practical insights in a vehicular network, we have used a commercial ray-tracing tool [28] and evaluated the proposed algorithms.

Notations: All boldface lower case and upper-case letters represent vectors and matrices, respectively, and calligraphy letters represent sets. The notation $\mathbb{C}^M$ denotes the set of complex M-dimensional vectors, $\mathbb{C}^{M\times N}$ denotes the set of complex $M\times N$ sized matrices, $|x|$ denotes the absolute value of scalar x and $\|\boldsymbol{x}\|$ denotes the l_2-norm of vector $\boldsymbol{x}$. The notation $\mathcal{CN}(\mu, N_0)$ denotes the complex circular Gaussian distribution with mean μ and variance N_0. The superscripts $()^H$ and $()^T$ are used to denote the Hermitian transpose and the transpose of a matrix, and $()^*$ denotes the complex conjugate. Further, the notation $\text{diag}(\boldsymbol{x})$ denotes a diagonal matrix constructed from the vector $\boldsymbol{x}$.

II. SYSTEM MODEL AND PROBLEM FORMULATION

We consider a vehicular communication system with K users and we label each user with an integer value $k = 1, \ldots, K$. We assume that the BS is equipped with M antennas and each vehicle has a single antenna. An RIS with N reflecting elements is introduced to assist the communication. Network is assumed to be communicating in time slots where normalized time slot $t \in \{0, 1, \ldots, \}$. Furthermore, we assume that all the users are communicating simultaneously in each time slot.

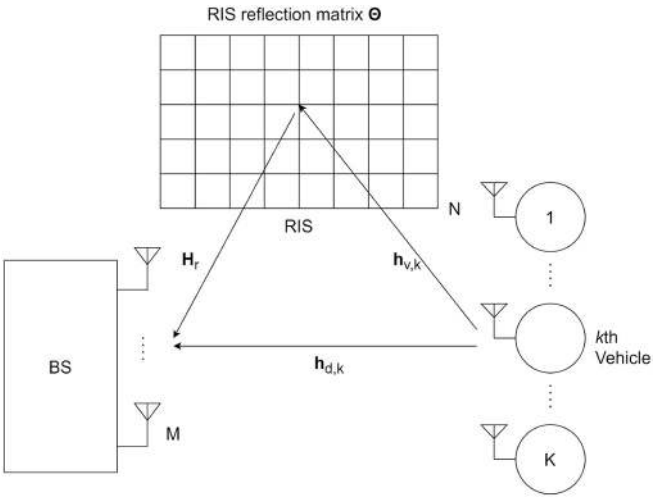

FIGURE 1. System model for RIS assisted uplink.

The signal transmitted by the kth user during time slot t is given by

$$x_k(t) = \sqrt{p_k} m_k(t), \tag{1}$$

where $m_k(t) \in \mathbb{C}$ represent the information bearing symbol and p_k is the transmit power of the kth user. We assume that information bearing symbols are normalized such that $E[|m_k(t)|^2] = 1$, therefore, $E[|x_k(t)|^2] = p_k$. Furthermore, we assume that all the users transmit their signals independently, resulting $E[x_j(t)x_k^*(t)] = 0$ when $j \neq k$.

The channel from each vehicle to the BS consists of 3 components. The channel from vehicle to RIS, channel from RIS to BS and the direct channel from vehicle to BS. Out of these channels, the channel from RIS to BS is common for all the users. Let $\boldsymbol{H}_r \in \mathbb{C}^{M\times N}$ be the channel between the RIS and BS, $\boldsymbol{h}_{v,k} \in \mathbb{C}^N$ be the channel between the kth vehicle and RIS, and $\boldsymbol{h}_{d,k} \in \mathbb{C}^M$ be the direct channel between the kth vehicle and BS, for $k = 1, \ldots, K$. The system model is shown in Fig. 1 depicting the channels of the kth vehicle.

When the incoming signals reach the RIS, each reflecting element of the RIS induces a phase shift to the signal and scatter it back to the BS. We assume that the amplitude of the signal does not change over the range of phase shifts. We consider these phase shifts to be one of L discrete levels. For simplicity, we assume these phase shifts take one of the values obtained by uniformly quantizing the interval $[0, 2\pi)$. Thus, the set of discrete phase shifts for each reflecting element is given by

$$\mathcal{F} = \{0, \Delta\theta, \ldots, (L-1)\Delta\theta\}, \tag{2}$$

where $\Delta\theta = 2\pi/L$. Let the, phase shifts of nth reflector of RIS be, $\theta_n \in \mathcal{F}$.

The effective channel from vehicle to BS utilizing the nth reflecting element can be expressed as

$$\boldsymbol{g}_n = \exp(j\theta_n)\boldsymbol{H}_r^{(n)} h_{v,k}^{(n)}, \tag{3}$$

where $\boldsymbol{H}_r^{(n)}$ is the nth column of $\boldsymbol{H}_r$ and $h_{v,k}^{(n)}$ is the nth element of the vector $\boldsymbol{h}_{v,k}$. All the reflecting elements of the RIS scatter the incoming signal in a similar manner. The received signal for a certain user consists of the sum of all the signal paths. The received signal of the kth user consisting of reflection signal paths and the direct path can be expressed as

$$y_k = \left(\sum_{n=1}^{N} \exp(j\theta_n)\boldsymbol{H}_r^{(n)} h_{v,k}^{(n)} + \boldsymbol{h}_{d,k}\right) x_k, \tag{4}$$

without considering the receiver noise. In-order to express this in a more compact form we denote the reflection matrix of the RIS by the diagonal matrix $\boldsymbol{\Theta}$, where $\boldsymbol{\Theta} = \text{diag}([\exp(j\theta_1), \exp(j\theta_2), \ldots, \exp(j\theta_N)]^T)$. The received signal at the BS consists of the sum of the signals from all the users. This can be expressed as

$$\boldsymbol{y} = \sum_{k=1}^{K} \left(\boldsymbol{H}_r \boldsymbol{\Theta} \boldsymbol{h}_{v,k} + \boldsymbol{h}_{d,k}\right) x_k + \boldsymbol{n}, \tag{5}$$

where $\boldsymbol{n} = [n_1, n_2, \ldots, n_M]$ with $n_m \sim \mathcal{CN}(0, N_0)$ being the complex additive white Gaussian noise (AWGN) at BS antennas.

The BS applies a linear beamforming vector $\boldsymbol{w}_k \in \mathbb{C}^M$ to decode kth user's message x_k, the decoded symbol is

$$\hat{y}_k = \sum_{k=1}^{K} \boldsymbol{w}_k^H \left(\boldsymbol{H}_r \boldsymbol{\Theta} \boldsymbol{h}_{v,k} + \boldsymbol{h}_{d,k}\right) x_k + \boldsymbol{w}_k^H \boldsymbol{n}, \text{ for } k = 1, \ldots, K. \tag{6}$$

Let us define $\boldsymbol{\Phi}_k = \boldsymbol{H}_r \text{diag}(\boldsymbol{h}_{v,k})$ and $\boldsymbol{v} = [\exp(j\theta_1), \exp(j\theta_2), \ldots, \exp(j\theta_N)]^T$. For notational simplicity, we also define $\boldsymbol{h}_{d,k} = \boldsymbol{b}_k$. Then, the decoded signal for the kth vehicle can be equivalently represented as

$$\hat{y}_k = \sum_{k=1}^{K} \boldsymbol{w}_k^H (\boldsymbol{\Phi}_k \boldsymbol{v} + \boldsymbol{b}_k) x_k + \boldsymbol{w}_k^H \boldsymbol{n}, \text{ for } k = 1, \ldots, K. \tag{7}$$

We assume that beamforming vectors at the BS are unit vectors, i.e., $\|\boldsymbol{w}_k\|^2 = 1$, for $k = 1, 2, \ldots, K$. Then SINR for the signal of the kth vehicle received at the BS can be written as

$$\text{SINR}_k = \frac{p_k |\boldsymbol{w}_k^H (\boldsymbol{\Phi}_k \boldsymbol{v} + \boldsymbol{b}_k)|^2}{\sum_{j\neq k} p_j |\boldsymbol{w}_k^H (\boldsymbol{\Phi}_j \boldsymbol{v} + \boldsymbol{b}_j)|^2 + N_0}. \tag{8}$$

Using the SINR expression in (8), the achievable rate for kth vehicle can be expressed as

$$R_k = \log(1 + \text{SINR}_k) \text{bit/s/Hz}, \text{ for } k = 1, \ldots, K. \tag{9}$$

Let $\boldsymbol{W} = [\boldsymbol{w}_1, \ldots, \boldsymbol{w}_K]$ and $\boldsymbol{p} = [p_1, \ldots, p_K]$. For this setup the WSR can be expressed as

$$f_0(\boldsymbol{v}, \boldsymbol{p}, \boldsymbol{W}) = \sum_{k=1}^{K} u_k R_k, \tag{10}$$

where u_k is the weight associated with the kth user.

Now the optimization problem can be formulated as follows,

$$\begin{aligned} &\text{maximize} \quad f_0(\boldsymbol{v}, \boldsymbol{p}, \boldsymbol{W}) \\ &\text{subject to} \quad v_i \in \mathcal{V}, \text{ for } i = 1, \ldots, N \\ &\qquad\qquad p_k \leq P_{\max}, \text{ for } k = 1, \ldots, K \\ &\qquad\qquad \|\boldsymbol{w}_k\|^2 = 1, \text{ for } k = 1, \ldots, K, \end{aligned} \tag{11}$$

where v_i for all $i = 1, 2, \ldots, N$, p_k for all $k = 1, 2, \ldots, K$ and $\boldsymbol{w}_k$ for all $k = 1, 2, \ldots, K$ are the optimization variables. Here, $P_{\max}$ is the maximum transmit power level allowed for the users and $\mathcal{V}$ is the set of discrete reflection coefficients corresponding to the set of discrete phase shifts $\mathcal{F}$, i.e.,

$$\mathcal{V} = \{\exp(j\theta) | \theta \in \mathcal{F}\}. \tag{12}$$

A. SINGLE USER ACHIEVABLE RATE MAXIMIZATION

Optimization problem (11) considers the joint optimization of transmit powers of the users, receiver filtering coefficients and phase shifts at the RIS. In order to get insights into the phase optimization aspects, we first consider the single user rate maximization problem. We denote the channel between vehicle and RIS by $\boldsymbol{h}_v \in \mathbb{C}^N$ and the direct channel between the vehicle and BS by $\boldsymbol{h}_d \in \mathbb{C}^M$. The channel from RIS to BS is denoted same as before.

In the single vehicle scenario, we do not have any interference, therefore we can set the transmit power $P = P_{\max}$. We set the receiver filtering coefficients using maximal ratio combining (MRC), which is optimal for single user case, i.e.,

$$\boldsymbol{w} = \frac{\boldsymbol{H}_r \boldsymbol{\Theta} \boldsymbol{h}_v + \boldsymbol{h}_d}{\|\boldsymbol{H}_r \boldsymbol{\Theta} \boldsymbol{h}_v + \boldsymbol{h}_d\|}. \tag{13}$$

Now the signal to noise ratio (SNR) can be written as

$$\text{SNR} = \frac{P\|\boldsymbol{H}_r \boldsymbol{\Theta} \boldsymbol{h}_v + \boldsymbol{h}_d\|^2}{N_0}. \tag{14}$$

Using the SNR expression (14) the achievable rate can be expressed as

$$R = \log\left(1 + \frac{P\|\boldsymbol{H}_r \boldsymbol{\Theta} \boldsymbol{h}_v + \boldsymbol{h}_d\|^2}{N_0}\right) \text{bit/s/Hz}. \tag{15}$$

As we see from (15), the achievable rate is dependent on the phase shifts at the RIS. Therefore, it should be possible to achieve higher rates by properly tuning the reflection matrix. This is known as passive beamforming or phase optimization. We consider the phase optimization problem at the RIS, where the achievable rate is maximized by choosing the optimum discrete phase shifts, i.e.,

$$\begin{aligned} &\text{maximize} \quad R \\ &\text{subject to} \quad v_i \in \mathcal{V}, \quad \text{for } i = 1, 2, \ldots, N, \end{aligned} \tag{16}$$

where v_i for all $i = 1, 2, \ldots, N$ are the optimization variables.

III. ALGORITHM DEVELOPMENT FOR SINGLE USER COMMUNICATIONS

In single user scenario we focus on finding the optimal phase shifts that maximize the rate as given in optimization problem (16). This problem is non-convex because of the discrete phase shifts and the nature of the objective function. It is possible to use exhaustive search to obtain the optimal solution. This means that the algorithm must go through N^L possibilities to obtain the optimal solution, which is computationally infeasible for large reflecting arrays. However, it is possible to develop a simple algorithm based on successive refinement [6].

Let us define $\boldsymbol{\Phi} = \boldsymbol{H}_r \text{diag}(\boldsymbol{h}_v)$ and $\boldsymbol{v} = [\exp(j\theta_1), \exp(j\theta_2), \ldots, \exp(j\theta_N)]^T$. Also, let $\boldsymbol{A} = \boldsymbol{\Phi}^H \boldsymbol{\Phi}$ and $\boldsymbol{b} = \boldsymbol{\Phi}^H \boldsymbol{h}_d$. RIS provides us with a way to control the channel conditions in a favorable way. We can increase the user rate by improving the channel gain. Let us examine the channel gain expression by expanding it. The channel gain is given by

$$\begin{aligned} \|\boldsymbol{H}_r \boldsymbol{\Theta} \boldsymbol{h}_v + \boldsymbol{h}_d\|^2 &= \|\boldsymbol{\Phi}\boldsymbol{v} + \boldsymbol{h}_d\|^2 \\ &= (\boldsymbol{\Phi}\boldsymbol{v} + \boldsymbol{h}_d)^H (\boldsymbol{\Phi}\boldsymbol{v} + \boldsymbol{h}_d) \\ &= \boldsymbol{v}^H \boldsymbol{A} \boldsymbol{v} + 2Re\left\{\boldsymbol{v}^H \boldsymbol{b}\right\} + \|\boldsymbol{h}_d\|^2. \end{aligned} \tag{17}$$

We can further simplify this expression by focusing on a single reflecting element. We focus on the nth reflecting element, keeping all the other reflecting elements $i \neq n$ fixed. The simplified channel gain expression is given by

$$2Re\left\{v_n^* \kappa_n\right\} + \tau_n, \tag{18}$$

where $\kappa_n = \sum_{j \neq n} A_{nj} v_j + b_n$ and $\tau_n = \sum_{j \neq n} \sum_{i \neq n} v_i^* A_{ij} v_j + 2Re\{\sum_{i \neq n} v_i^* b_i\} + A_{nn} + \|\boldsymbol{h}_d\|^2$. Here, A_{ij} and b_i represent the individual elements of $\boldsymbol{A}$ and $\boldsymbol{b}$ respectively.

We see that expression (18) is linear in terms of v_n, and we know that the product of two complex quantities are maximized when they are in phase. This enable us to find the optimal phase shift for the nth reflector simply with a linear search over discrete phase shift levels. Thus, the optimal phase shift of the nth reflecting element is given by

$$\theta_n^{\text{opt}} = \arg\min_{\theta \in \mathcal{F}} |\theta - \angle \kappa_n|. \tag{19}$$

Similarly, we can set the phase shifts of all the reflecting elements. We do this in N steps optimizing a single reflecting element at a time. We can express this procedure in Algorithm 1.

A. EFFICIENT PHASE OPTIMIZATION SCHEMES

The phase optimization Algorithm 1 depends on the availability of full CSI for all the channels involved. An RIS consists of large number of passive reflecting elements. When utilizing the RIS, we need to estimate the channel through each reflecting element in addition to the channel between the vehicle and BS. Since reflecting elements are not active, we need to depend on the pilots received at the BS for channel estimation. We need to allocate a lot of

Algorithm 1: Successive Refinement Algorithm

initialization: set $\boldsymbol{\Theta} = \boldsymbol{\Theta}^{(0)}$, set $R^{(0)} = 0$, set $k = 1$, set $R^{(k)}$ using equation (15)
while $|R^{(k)} - R^{(k-1)}| > \epsilon$ **do**
  for n=*1 to* N **do**
    set θ_n using equation (19)
  end
  $k = k + 1$
  set $R^{(k)}$ using equation (15)
end

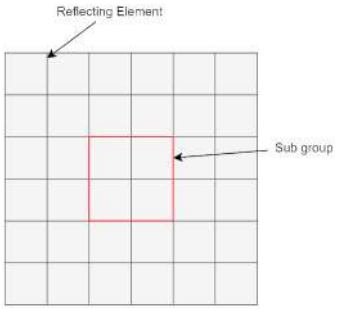

FIGURE 2. Reflect array divided into subgroups.

resources in order to estimate all the channels. Therefore, it is important to investigate on ways to reduce this channel estimation overhead. In the next 2 sections we will introduce two phase optimization schemes that reduce the channel estimation overhead.

1) GROUPING-BASED RIS PHASE OPTIMIZATION

The reflecting elements in the RIS are arranged in a planar array. We can group these elements together based on the adjacency. After dividing the reflecting elements into subgroups, we consider a subgroup as a single unit. We perform channel estimation on subgroup basis instead of element wise, resulting only one channel estimate for each subgroup. Also, the phase optimization algorithm is performed subgroup wise. Later, phase shifts of all the reflecting elements in the subgroup are set to the same value for the subgroup. This reduces the number of channels we need to estimate considerably. For simplicity we consider uniform grouping of reflecting elements.

For example, Fig. 2 shows a reflecting array consisting of 6×6 reflecting elements. It is divided into 2×2 sized subgroups. Each subgroup is considered as a single reflecting element. Therefore, passive beamforming is effectively done for a 3×3 reflecting array. This reduces the channel estimation overhead as well as the complexity of the successive refinement algorithm. After the phase shifts are found, phase shifts of all the reflectors in the group are set to the same value for the subgroup.

2) POSITION-BASED PASSIVE BEAMFORMING

The directional angles change much slower than change of CSI in the mmWave frequency band [29]. The position and velocity can be used to determine the beam direction of a vehicle undergoing vehicle to infrastructure (V2I) communication [30]. LoS links are prominent in this scenario [30]. Therefore, the system should be able to perform beamforming solely based on LoS links. We can assume that BS tracks the vehicle position, velocity, and also the arrival and departure angles. Then, the LoS channel can be calculated from this information. Assuming planar arrays at both the BS and RIS, the LoS channel between BS and RIS can be expressed as,

$$\boldsymbol{H}_{r,los} = \sqrt{L_{los}} \exp\left(\frac{-j2\pi d}{\lambda}\right) \boldsymbol{a}_{bs}\left(\phi^{bs}, \theta^{bs}\right) \boldsymbol{a}_{irs}^{H}\left(\phi^{irs}, \theta^{irs}\right), \tag{20}$$

where d is the distance between BS and RIS, $\boldsymbol{a}_{bs}(\phi^{bs}, \theta^{bs}) \in \mathbb{C}^M$ is the array response of BS for the considered azimuth and elevation arrival angles, and $\boldsymbol{a}_{irs}(\phi^{irs}, \theta^{irs}) \in \mathbb{C}^N$ is the array response of RIS for the considered azimuth and elevation departure angles. Similarly, $\boldsymbol{h}_{v,los}$ and $\boldsymbol{h}_{d,los}$ can be defined. In order to obtain full CSI, we need to estimate the channels through each reflecting element. Here, we need to only estimate the arrival and departure angles for the whole array along with the position and velocity of the vehicle. Therefore, this takes less overhead. After the LoS channel is estimated the system can then perform passive beamforming.

IV. ALGORITHM DEVELOPMENT FOR MULTI-USER COMMUNICATIONS

Compared to the optimization problem for single user communication, the optimization problem for multi-user communication is more complex. Now, the interference between users must be taken into account. User power allocation problem must be tackled in addition to phase optimization and receive filtering. Also, the phase shifts at the RIS must be optimized considering all the users.

The optimization problem described in (11) is non-convex due to discrete phase shifts and also because of the composition of objective function. Yet, we can decompose the original problem into a more tractable form by applying the FP techniques presented in [26]. We were inspired by the work presented in [25]. However, our optimization problem is different since we consider uplink and an RIS with discrete phase shifts. Also, we consider more general update rules instead of BCD based update rules. First, we will introduce the two FP transformations that we will use to reformulate our problem.

A. FP TECHNIQUES

1) LAGRANGIAN DUAL TRANSFORM

Consider the following optimization problem of maximizing the sum rate.

$$\begin{aligned} &\text{maximize} \quad \sum_{k=1}^{K} \log(1 + \gamma_k(\boldsymbol{x})) \\ &\text{subject to} \quad \boldsymbol{x} \in \boldsymbol{\mathcal{X}}, \end{aligned} \tag{21}$$

where $\gamma_k(\boldsymbol{x})$ is the SINR with $\boldsymbol{x}$ being the optimization variable with domain $\boldsymbol{\mathcal{X}}$, where $\boldsymbol{\mathcal{X}}$ is the feasible set. By introducing auxiliary variables $\boldsymbol{\alpha} = [\alpha_1, \ldots, \alpha_k]^T$, it can be shown that problem (21) can be equivalently represented as [26],

$$\begin{aligned} \text{maximize} \quad & \sum_{k=1}^{K} \log(1+\alpha_k) - \alpha_k + (1+\alpha_k)\frac{\gamma_k(\boldsymbol{x})}{1+\gamma_k(\boldsymbol{x})} \\ \text{subject to} \quad & \boldsymbol{x} \in \boldsymbol{\mathcal{X}} \\ & \alpha_k \geq 0, \text{ for k=1,..., K}, \end{aligned} \tag{22}$$

where $\boldsymbol{x}$ and $\boldsymbol{\alpha}$ are the optimization variables. This transform has enabled us to take the SINR expression out of the logarithm. We can easily verify the equivalence of expressions (21) and (22) by substituting $\alpha_k = \gamma_k(\boldsymbol{x})$ in (22). For given $\boldsymbol{\alpha}$, the problem (22) reduces to a SINR maximization problem.

2) QUADRATIC TRANSFORM

Note that our SINR expression in (8) can be represented in the form $\frac{|A(\boldsymbol{x})|^2}{B(\boldsymbol{x})}$. Then, we can formulate the SINR maximization problem as,

$$\begin{aligned} \text{maximize} \quad & \sum_{k=1}^{K} \frac{|A_k(\boldsymbol{x})|^2}{B_k(\boldsymbol{x})} \\ \text{subject to} \quad & \boldsymbol{x} \in \boldsymbol{\mathcal{X}}, \end{aligned} \tag{23}$$

where $\boldsymbol{x}$ is the optimization variable. By introducing auxiliary variables $\boldsymbol{\beta} = [\beta_1, \ldots, \beta_k]^T$, this problem is equivalently represented as [26],

$$\begin{aligned} \text{maximize} \quad & \sum_{k=1}^{K} 2Re\left\{\beta_k^* A_k(\boldsymbol{x})\right\} - |\beta_k|^2 B_k(\boldsymbol{x}) \\ \text{subject to} \quad & \boldsymbol{x} \in \boldsymbol{\mathcal{X}}, \end{aligned} \tag{24}$$

where $\boldsymbol{x}$ and $\boldsymbol{\beta}$ are the optimization variables. With these results, we are now ready to reformulate our optimization problem in a different form.

B. PROBLEM REFORMULATION

First, let us apply the Lagrangian dual transform (22) defined in the last section to our original problem. This results in the new objective function,

$$\begin{aligned} f_1(\boldsymbol{\theta}, \boldsymbol{p}, \boldsymbol{W}, \boldsymbol{\alpha}) = & \sum_{k=1}^{K} u_k \log(1+\alpha_k) - \sum_{k=1}^{K} u_k \alpha_k \\ & + \sum_{k=1}^{K} \frac{u_k(1+\alpha_k)|\boldsymbol{w}_k^H(\boldsymbol{\Phi}_k \boldsymbol{v} + \boldsymbol{b}_k)|^2 p_k}{\sum_{j=1}^{K} |\boldsymbol{w}_k^H(\boldsymbol{\Phi}_j \boldsymbol{v} + \boldsymbol{b}_j)|^2 p_j + N_0}. \end{aligned} \tag{25}$$

Next, we apply the quadratic transform (24) defined in the last section. The resulting objective function can be written as,

$$\begin{aligned} & f_2(\boldsymbol{v}, \boldsymbol{p}, \boldsymbol{W}, \boldsymbol{\alpha}, \boldsymbol{\beta}) \\ & = \sum_{k=1}^{K} u_k \log(1+\alpha_k) - \sum_{k=1}^{K} u_k \alpha_k \\ & \quad + \sum_{k=1}^{K} 2\sqrt{u_k(1+\alpha_k)p_k} Re\left\{\beta_k^* \boldsymbol{w}_k^H(\boldsymbol{\Phi}_k \boldsymbol{v} + \boldsymbol{b}_k)\right\} \\ & \quad - \sum_{k=1}^{K} |\beta_k|^2 \left(\sum_{j=1}^{K} |\boldsymbol{w}_k^H(\boldsymbol{\Phi}_j \boldsymbol{v} + \boldsymbol{b}_j)|^2 p_j + N_0 \right). \end{aligned} \tag{26}$$

The optimization problem (11) can now be represented as follows,

$$\begin{aligned} \text{maximize} \quad & f_2(\boldsymbol{v}, \boldsymbol{p}, \boldsymbol{W}, \boldsymbol{\alpha}, \boldsymbol{\beta}) \\ \text{subject to} \quad & v_i \in \mathcal{V}, \text{ for } i = 1, 2, \ldots, N \\ & p_k \leq P_{\max}, \text{ for } k = 1, \ldots, K \\ & \|\boldsymbol{w}_k\|^2 = 1, \text{ for } k = 1, \ldots, K \\ & \alpha_k \geq 0, \text{ for } k = 1, \ldots, K, \end{aligned} \tag{27}$$

where $\boldsymbol{v}, \boldsymbol{p}, \boldsymbol{W}, \boldsymbol{\alpha}$ and $\boldsymbol{\beta}$ are the optimization variables. Still, this problem is non-convex due to the form of the objective function and discrete reflection coefficients. The optimization variables are tightly coupled. However, now this problem is analytically more tractable.

C. ALTERNATING OPTIMIZATION ALGORITHM

We tackle the optimization problem (27) by using alternating optimization of variables. Here, we optimize one variable at a time, keeping the other variables constant. We update the optimization variables $\boldsymbol{v}, \boldsymbol{p}, \boldsymbol{W}, \boldsymbol{\alpha}$, and $\boldsymbol{\beta}$ in 5 steps.

1) UPDATING AUXILIARY VARIABLES

The auxiliary variables $\boldsymbol{\alpha}$ and $\boldsymbol{\beta}$ can be updated based on the values of $\boldsymbol{v}, \boldsymbol{p}$, and $\boldsymbol{W}$. An update rule can be derived by setting the partial derivatives $\frac{\partial f_1}{\partial \alpha_k}$ and $\frac{\partial f_2}{\partial \beta_k}$ to zero. Thus, the update rules can be expressed as

$$\alpha_k = \frac{\bar{p_k}\left|\bar{\boldsymbol{w}_k}^H(\boldsymbol{\Phi}_k \bar{\boldsymbol{v}} + \boldsymbol{b}_k)\right|^2}{\sum_{j \neq k} \bar{p_j}\left|\bar{\boldsymbol{w}_k}^H(\boldsymbol{\Phi}_j \bar{\boldsymbol{v}} + \boldsymbol{b}_j)\right|^2 + N_0}, \tag{28}$$

and

$$\beta_k = \frac{\sqrt{u_k(1+\bar{\alpha_k})\bar{p_k}}\bar{\boldsymbol{w}_k}^H(\boldsymbol{\Phi}_k \bar{\boldsymbol{v}} + \boldsymbol{b}_k)}{\sum_{j=1}^{K} \bar{p_j}\left|\bar{\boldsymbol{w}_k}^H(\boldsymbol{\Phi}_j \bar{\boldsymbol{v}} + \boldsymbol{b}_j)\right|^2 + N_0}. \tag{29}$$

Note that α_k it the SINR of the kth user. Therefore, it will always be a real positive number and it will satisfy the positive constraint in the optimization problem (27). Here, β_k corresponds to the decoded symbol of the kth user and it is normalized by a number that depend on total signal, interference and noise power.

Algorithm 2: Receiver Filter Update Algorithm for kth User

initialization: $\mu_k^{\text{upper}}, \mu_k^{\text{lower}}$
while $\mu_k = (\mu_k^{upper} + \mu_k^{lower})/2$
$\mu_k^{upper} - \mu_k^{lower} > \epsilon_1$ *And* $|\|\boldsymbol{w}_k\| - 1| > \epsilon_2$ **do**
  update $\boldsymbol{w}_k$ using equation (31)
  if $\|\boldsymbol{w}_k\| > 1$ **then**
    $\mu_k^{\text{lower}} = \mu_k$
  else
    $\mu_k^{\text{upper}} = \mu_k$
  end
end

2) UPDATING RECEIVER FILTER

The optimum receiver filter coefficients $\boldsymbol{W}$ are found using the current values of the other optimization variables $\boldsymbol{v}, \boldsymbol{p}, \boldsymbol{\alpha}$ and $\boldsymbol{\beta}$. This optimization problem can be expressed as

$$\begin{aligned} &\text{maximize } f_1\big(\bar{\boldsymbol{v}}, \bar{\boldsymbol{p}}, \boldsymbol{W}, \bar{\boldsymbol{\alpha}}, \bar{\boldsymbol{\beta}}\big) \\ &\text{subject to } \|\boldsymbol{w}_k\|^2 = 1, \text{for } k = 1, \ldots, K, \end{aligned} \tag{30}$$

where $\boldsymbol{W}$ is the optimization variable. The optimization problem (30) has been studied extensively in the literature. We can find a stationary solution to this problem by solving the Lagrangian dual problem [31], and thus have

$$\boldsymbol{w}_k = \sqrt{u_k(1+\bar{\alpha_k})}\bar{p_k}\bar{\beta_k}\left(\mu_k \boldsymbol{I}_M + |\bar{\beta_k}|^2 \sum_{j=1}^{K} \bar{p_j}\bar{\boldsymbol{h_j}}\bar{\boldsymbol{h_j}}^H\right)^{-1}\bar{\boldsymbol{h}_k}, \tag{31}$$

where $\bar{\boldsymbol{h}_j} = \boldsymbol{\Phi}_j\bar{\boldsymbol{v}} + \boldsymbol{b}_j$ and μ_k is the optimal dual variable such that the unit gain constraint for receiver filter coefficient $\boldsymbol{w}_k$ is satisfied. We can search for the dual variable efficiently through bisection [31] method. Algorithm 2 expresses the calculation of $\boldsymbol{w}_k$ based on the bisection method. Here, ϵ_1 and ϵ_2 are the error tolerances for the algorithm.

3) UPDATING TRANSMIT POWER OF USERS

We consider the uplink power control problem based on the current values of the optimization variables $\boldsymbol{v}, \boldsymbol{W}, \boldsymbol{\alpha}$, and $\boldsymbol{\beta}$. This optimization problem can be expressed as

$$\begin{aligned} &\text{maximize } f_2\big(\bar{\boldsymbol{v}}, \boldsymbol{p}, \bar{\boldsymbol{W}}, \bar{\boldsymbol{\alpha}}, \bar{\boldsymbol{\beta}}\big) \\ &\text{subject to } p_k \le P_{\max}, \text{for } k = 1, \ldots, K, \end{aligned} \tag{32}$$

where p_k, for $k = 1, \ldots, K$ are the optimization variables. We find the optimum power coefficients by setting partial derivatives $\frac{\partial f_2}{\partial p_k}$ for $k = 1, \ldots, K$ to zero. Thus the update rule for the power coefficients is

$$p_k = \min(\tilde{p_k}, P_{\max}), \tag{33}$$

where

$$\tilde{p_k} = u_k(1+\bar{\alpha_k})\left[\frac{Re\left\{\bar{\beta_k}^* \bar{\boldsymbol{w}_k}^H(\boldsymbol{\Phi}_k\bar{\boldsymbol{v}} + \boldsymbol{b}_k)\right\}}{\sum_{j=1}^{K}|\bar{\beta_j}|^2|\bar{\boldsymbol{w}_j}^H(\boldsymbol{\Phi}_k\bar{\boldsymbol{v}} + \boldsymbol{b}_k)|^2}\right]^2, \tag{34}$$

for $k = 1, \ldots, K$.

4) PHASE OPTIMIZATION

Based on the current values of other optimization variables we can consider the phase optimization problem. Let us define $\boldsymbol{c}_{j,k} = \boldsymbol{w}_k^H\boldsymbol{\phi}_j$ and $d_{j,k} = \boldsymbol{w}_k^H\boldsymbol{b}_j$. We can rewrite the optimization problem after dropping all the irrelevant terms as

$$\begin{aligned} &\text{maximize } f_3(\boldsymbol{v}) \\ &\text{subject to } v_i \in \mathcal{V}, \text{for } i = 1, 2, \ldots, N, \end{aligned} \tag{35}$$

where $f_3(\boldsymbol{v}) = \boldsymbol{v}^H\boldsymbol{Q}\boldsymbol{v} + 2Re\{\boldsymbol{r}^H\boldsymbol{v}\}$ and $\boldsymbol{v}$ is the optimization variable. Here $\boldsymbol{Q}$ and $\boldsymbol{r}$ are defined as

$$\boldsymbol{Q} = -\sum_{k=1}^{K}|\bar{\beta_k}|^2\sum_{j=1}^{K}\bar{\boldsymbol{c}_{j,k}}^H\bar{\boldsymbol{c}_{j,k}}, \tag{36}$$

and

$$\boldsymbol{r} = \sum_{k=1}^{K}\left[\sqrt{u_k(1+\bar{\alpha_k})}\bar{p_k}\bar{\beta_k}\bar{\boldsymbol{c}_{k,k}}^H - |\bar{\beta_k}|^2\sum_{j=1}^{K}\bar{d_{j,k}}\bar{\boldsymbol{c}_{j,k}}^H\right]. \tag{37}$$

Optimization problem (35) is still non-convex due to discrete phase shifts. It is possible to find the optimal solution by brute force. However, this is not feasible for large reflecting arrays, because the algorithm has to go through N^L possibilities. However, note that the objective function $f_3(\boldsymbol{v})$ has the same form as the expression (17). Therefore, we can alternatively optimize the phase shift of each reflecting element individually keeping the other elements fixed. This will yield a sub-optimal solution with much lower complexity. We can focus on a single reflecting element, v_n considering all the other reflecting elements (v_i, $i \neq n$) fixed. We can write the objective function as

$$f_4(\boldsymbol{v}) = 2Re\big\{v_n^*\kappa_n\big\} + \tau_n, \tag{38}$$

where $\kappa_n = \sum_{j\neq n}Q_{n,j}v_j + r_n$ and $\tau_n = \sum_{j\neq n}\sum_{i\neq n}v_i^*Q_{i,j}v_j + 2Re\{\sum_{i\neq n}v_i^*r_i\} + Q_{n,n}$. Here, $Q_{i,j}$ and r_i represent the individual elements of $\boldsymbol{Q}$ and $\boldsymbol{r}$ respectively. The optimal phase shift of each reflecting element can be obtained as

$$\theta_n^{\text{opt}} = \arg\min_{\theta\in\mathcal{F}}|\theta - \angle\kappa_n|. \tag{39}$$

We can formulate the successive refinement algorithm similar to algorithm 1. The complete alternating optimization algorithm steps can be stated as Algorithm 3. Here, ϵ_3 is the threshold that determine the convergence of the algorithm.

D. OPTIMIZATION WITHOUT RIS

We intend to evaluate the gains of RIS aided communication. Therefore, we need an algorithm to solve the optimization problem without RIS assistance, which can be stated as follows.

$$\begin{aligned} &\text{maximize } f_2(\boldsymbol{p}, \boldsymbol{W}, \boldsymbol{\alpha}, \boldsymbol{\beta}) \\ &\text{subject to } p_k \le P_{\max}, \text{for} k = 1, 2, \ldots, K \\ &\qquad \|\boldsymbol{w}_k\|^2 = 1, \text{for} k = 1, 2, \ldots, K \end{aligned}$$

Algorithm 3: Alternating Optimization Algorithm for RIS Aided Communications

initialization: $\boldsymbol{v}$, $\boldsymbol{p}$, $\boldsymbol{W}$, set $R^{(0)} = 0$, set $t = 1$, set $R^{(1)}$ with equation (10)
while $|R^{(t)} - R^{(t-1)}| > \epsilon_3$ **do**
  update α_k using equation (28) for all $k = 1, \ldots, K$
  update β_k using equation (29) for all $k = 1, \ldots, K$
  update $\boldsymbol{v}$ using Algorithm 1 with objective function (38))
  update $\boldsymbol{w}_k$ using Algorithm 2 for all $k = 1, \ldots, K$
  update p_k using equation (33) for all $k = 1, \ldots, K$
  $t = t + 1$
  calculate $R^{(t)}$ with equation (10)
end

$$\alpha_k \geq 0, \text{for} k = 1, 2, \ldots, K, \tag{40}$$

with

$$f_2(\boldsymbol{p}, \boldsymbol{W}, \boldsymbol{\alpha}, \boldsymbol{\beta}) = \sum_{k=1}^{K} u_k \log(1 + \alpha_k) - \sum_{k=1}^{K} u_k \alpha_k + \sum_{k=1}^{K} 2\sqrt{u_k(1+\alpha_k)} p_k Re\left\{\beta_k^* \boldsymbol{w}_k^H \boldsymbol{b}_k\right\} - \sum_{k=1}^{K} |\beta_k|^2 \left(\sum_{j=1}^{K} \left|\boldsymbol{w}_k^H \boldsymbol{b}_j\right|^2 p_j + N_0\right), \tag{41}$$

where $\boldsymbol{p}, \boldsymbol{W}, \boldsymbol{\alpha}$ and $\boldsymbol{\beta}$ are the optimization variables. This problem is also nonconvex due to the coupling of optimization variables in the objective function. However, we can use the same optimization procedure developed with RIS while discarding phase optimization. Algorithm 4 illustrates this procedure. Here, ϵ_4 is the error threshold of the algorithm that determines the convergence.

The problem reformulation with the FP technique has decoupled the signal and interference terms in the objective function, also, enabling the application of successive refinement. It has allowed the variables to exist in their original discrete form, thus avoiding the additional step of rounding to the closest discrete value. This is an efficient solution which is scalable with the number of reflecting elements.

V. NUMERICAL RESULTS

In this section, we evaluate the performance of the proposed algorithms and schemes. We consider two types of simulations, based on stochastic channel modeling and ray tracing using Wireless InSite [28]. In stochastic simulations we do not take mobility into account and perform the simulations using random channel realizations. Then, we carry out ray tracing simulations taking mobility into account. First, we present the results of single-user communication and then multi-user communications. Finally, we perform stochastic simulations using a time varying channel model to evaluate mobility.

In stochastic simulations, we use the Rician fading model for all the channels involved. In this model the channel matrix is given by,

$$\boldsymbol{H} = \frac{1}{\sqrt{\beta + 1}} \boldsymbol{H}_{nlos} + \sqrt{\frac{\beta}{\beta + 1}} \boldsymbol{H}_{los}, \tag{42}$$

where $\boldsymbol{H}_{nlos}$ consists of independent and identically distributed Rayleigh fading coefficients, $\boldsymbol{H}_{los}$ is the deterministic LoS component, and β is the Rician factor. Let β_r, β_v and β_d be the Rician factors for RIS-BS, vehicle-RIS and vehicle-BS links respectively. We use $\beta_r = \infty$, which corresponds to a pure LoS channel, $\beta_v = 1$, and $\beta_d = 0$, which corresponds to a non-LoS channel. To model path loss, 3GPP TR 38.901 UMi - Street Canyon path loss model [32] is used.

Algorithm 4: Alternating Optimization Algorithm Without RIS Assistance

initialization: $\boldsymbol{p}$, $\boldsymbol{W}$, set $R^{(0)} = 0$, set $t = 1$, set $R^{(t)}$ with equation (10)
while $|R^{(t)} - R^{(t-1)}| > \epsilon_4$ **do**
  update α_k using equation (28) for all $k = 1, \ldots, K$
  update β_k using equation (29) for all $k = 1, \ldots, K$
  update $\boldsymbol{w}_k$ using Algorithm 2 for all $k = 1, \ldots, K$
  update p_k using equation (33) for all $k = 1, \ldots, K$
  $t = t + 1$
  calculate $R^{(t)}$ with equation (10)
end

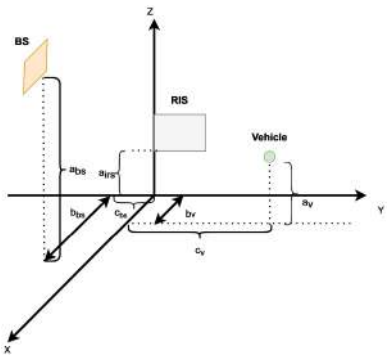

FIGURE 3. Device positions in the stochastic simulation.

A. SINGLE-USER COMMUNICATION

In this section, we evaluate the performance of algorithms developed in Section III.

1) STOCHASTIC SIMULATIONS

Fig. 3 shows the position of the devices in the stochastic simulation. BS is equipped with a 4×2 uniform planar array (UPA) antenna panel. RIS consists of a planar array of 16×16 passive reflecting elements. We consider a single antenna transmitter at the vehicle. RIS is placed on the YZ plane at a height $a_{irs} = 1$ m. BS is placed on the XZ plane at a height $a_{bs} = 2$ m and at distances of $b_{bs} = 20$ m, and $c_{bs} = 10$ m from the origin. Vehicle antenna is placed at a height $a_v = 1$ m and at distances of $b_v = 1.5$ m, and c_v from the origin.

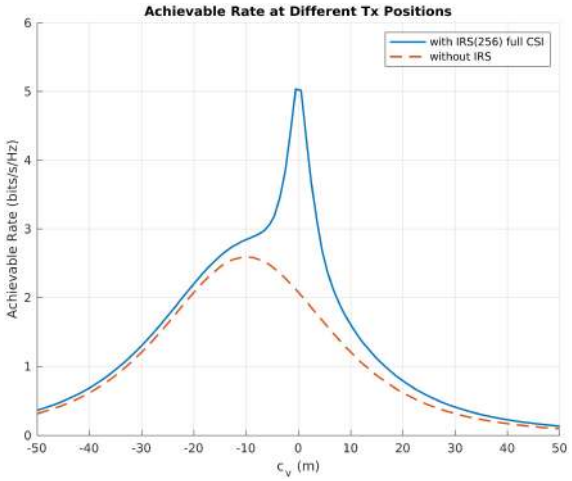

FIGURE 4. Variation of achievable rate as vehicle position is changed.

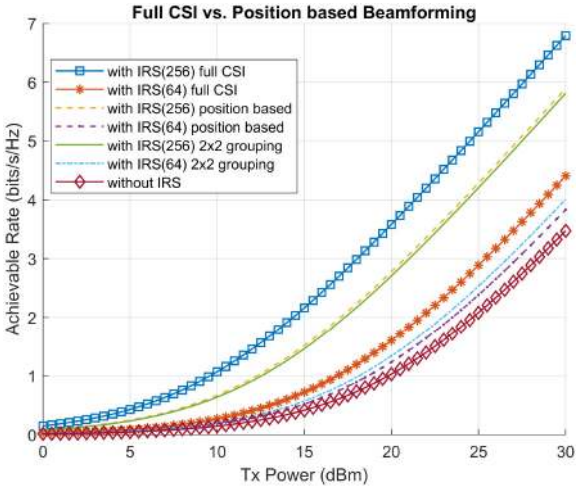

FIGURE 5. Comparison of variation of achievable rate with transmit power with grouping and position-based beamforming.

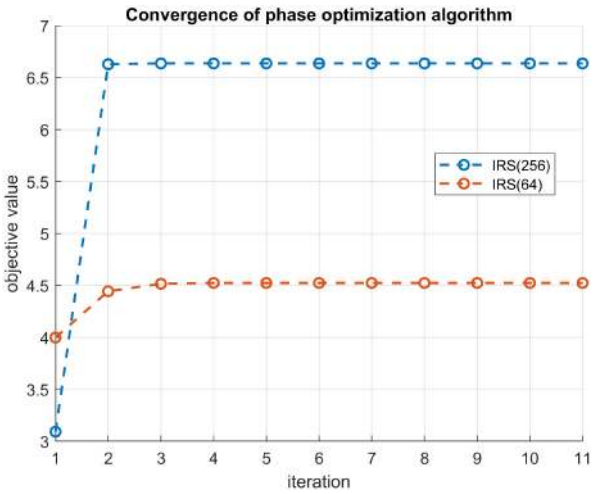

FIGURE 6. Convergence of the successive refinement algorithm.

The variation of the achievable rate while changing the position of the vehicle by changing c_v is shown in Fig. 4. It is obtained by averaging out over a large number of channel realizations. A significant increase in the achievable rate by utilizing the RIS is seen at the point $c_v = 0$, which is the closest point to the RIS. The performance improvement decreases as the vehicle moves further away from the RIS. Therefore, the vehicle needs to be in close proximity of the RIS in-order to get a significant benefit. Otherwise, the path loss will be severe, compromising the passive beamforming gain.

Next, the position of the vehicle is fixed at $c_v = 0$, which is the closest point to the RIS. The transmit power is changed and the achievable rate is observed for reconfigurable array sizes of 16×16 and 8×8. Two phase optimization schemes proposed in the last section are compared with full CSI results as shown Fig. 5. We can see that both schemes perform close to each other. However, for the 16×16 array, position-based beamforming is slightly better, and for the 8×8 array, grouping-based beamforming is better.

A degradation in the performance is observed when grouping is used instead of full CSI. However, there is still a significant performance gain by utilizing the RIS with grouping compared to performance without RIS. Also, it should be noted that, when a 16×16 reflecting array is used with 2×2 grouping, it effectively acts as an 8×8 panel in-terms of passive beamforming. This reduces the number of reflection paths to be estimated at the RIS by 75%. Yet, it provides a better performance than utilizing an 8×8 reflecting array with full CSI. Therefore, grouping facilitates the usage of large reflecting arrays while keeping the channel estimation overhead low.

The performance of position-based beamforming also shows a reduction compared to beamforming with full CSI. Nevertheless, it shows a good performance for the 16×16 array with only a small decrease in rate compared to full CSI. However, the performance of the 8×8 array is not satisfactory, and the rate curve lies closely to the rate curve without RIS. Therefore, position-based beamforming is more suitable for large reflecting arrays.

The convergence of the successive refinement based phase optimization algorithm for a single channel realization is shown in Fig. 6. We see that, the algorithm converges in just 3 iterations for 8×8 reflecting array. It converges in just 2 iterations for 16×16 array. Therefore, we can conclude that the algorithm converges fast for reflecting arrays of different sizes. Here, we have set the initial values of phase shifts to zero ($\theta_i = 0$, for all $i = 1, 2, \ldots, N$).

The effect of the number of discrete phase shift levels available at the RIS is illustrated in Fig. 7. It shows that using 1-bit phase shifts hardly provides any benefits to the existing communication. As we increase this to 2-bit, a dramatic increase in the performance is seen. However, there is only a slight performance improvement when we increase phase shift levels to 3-bit. Therefore, we can get a good performance just by utilizing a reflecting array with 2-bit

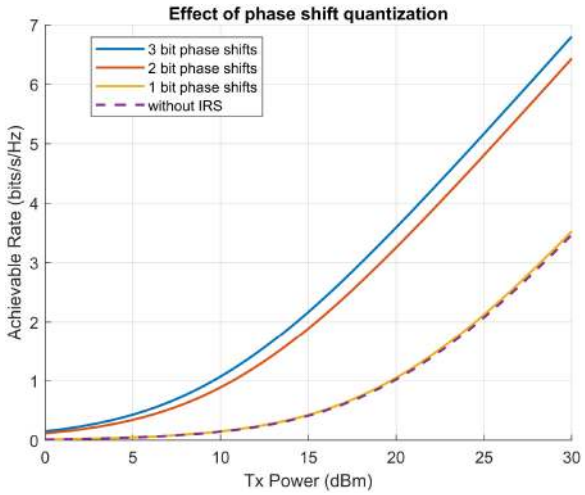

FIGURE 7. Illustrating the effects of quantizing the phase shifts.

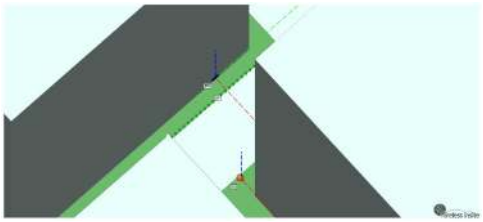

FIGURE 8. Simulating RIS aided system in Remcom Wireless InSite [28].

phase shifts. This is convenient since, the practical implementation of RISs allows only a limited number of discrete phase shift levels.

2) RAY TRACING SIMULATIONS

Stochastic simulations have provided us with many insights into RIS aided communications. However, they rely on simplified assumptions such as static conditions and a simple channel model, and mobility is not taken into account either. Since we focus on vehicular communications, we need to perform a more complex simulation to model mobility and the environmental conditions in detail. Ray tracing is considered as a reliable methodology to estimate complex propagation characteristics in mmWave vehicular networks [33].

Fig. 8 shows the vehicular communication system modeled in Remcom Wireless InSite [28]. Here, we consider an urban scenario with surrounding building and roads. The BS is placed at one side of the road. The RIS is placed at the other side of the road to improve the performance of the communication for a vehicle travelling closer to the RIS. The route of the vehicle is defined with an average speed of 10 m/s. Vehicular traffic is not considered for simplicity. We model the RIS as a rectangular array of patch antennas. We obtain the channel matrices after running the ray tracing simulation. Then we consider the closest point of the vehicle to the RIS and phase optimization is performed while changing the transmit power. Fig. 9 shows the variation of

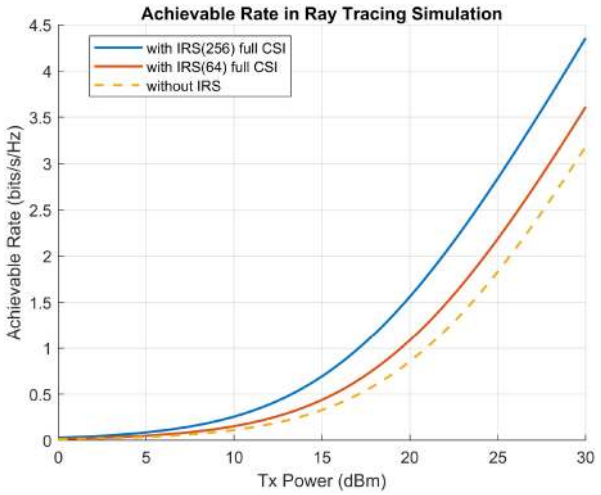

FIGURE 9. Variation of achievable rate with transmit power for the ray tracing simulation.

achievable rate with transmit power for reflecting array sizes of 8×8 and 16×16. There is a significant performance gain for the 16×16 reflecting array. However, the 8×8 array only shows a slight improvement over the communication without RIS. This suggests that large reflecting arrays are needed to improve the system performance considerably. As we have seen in earlier simulations, ray tracing also confirms the improvement to the communication provided by RIS.

B. MULTI-USER COMMUNICATIONS

In this section, we validate the algorithms developed in Section IV for multi-user communications. We consider two scenarios with different number of vehicles. All the scenarios in this section utilize an RIS with 16×16 reflecting elements to assist a BS with a 2×2 UPA antenna panel. We use following benchmarks in these simulations to compare the performance of the RIS aided system.

- Without RIS: We solve the optimization problem without considering the RIS with Algorithm 4 and calculate the performance.
- Randomized phase shifts: We run Algorithm 3 but use random phase shifts for the RIS at each step.
- Equal power allocation with MRC (EQP-MRC): We set equal power for the users with the maximum power level and use MRC for receive beamforming, while performing phase optimization with successive refinement.
- Random phase iteration: We perform phase optimization by setting the phases randomly. We repeat this process for a fixed number of iterations and select the phase shifts which give the maximum rate.
- Upper Bound: We run the Algorithm 3 for an extended period (100 iterations) and take the maximum WSR obtained as the upper bound.

Additionally, we evaluate the performance of position-based beamforming along with these benchmarks.

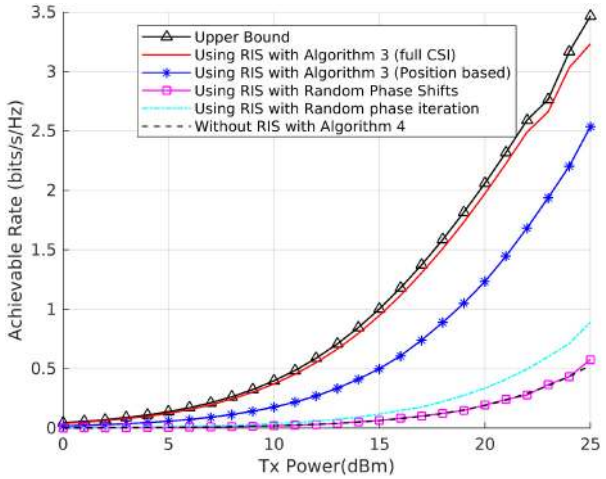

FIGURE 10. Variation of achievable rate with transmit power for $K = 1$.

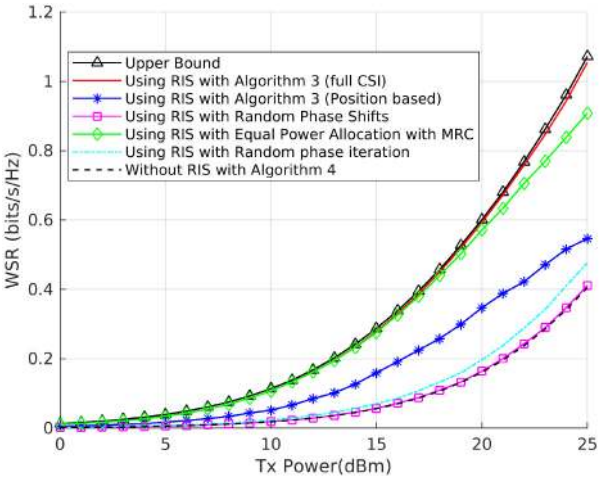

FIGURE 12. Variation of WSR with transmit power for $K = 4$.

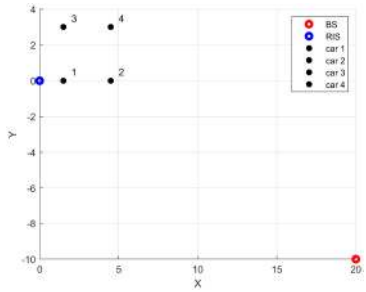

FIGURE 11. Position of vehicles for multi-user scenario with $K = 4$.

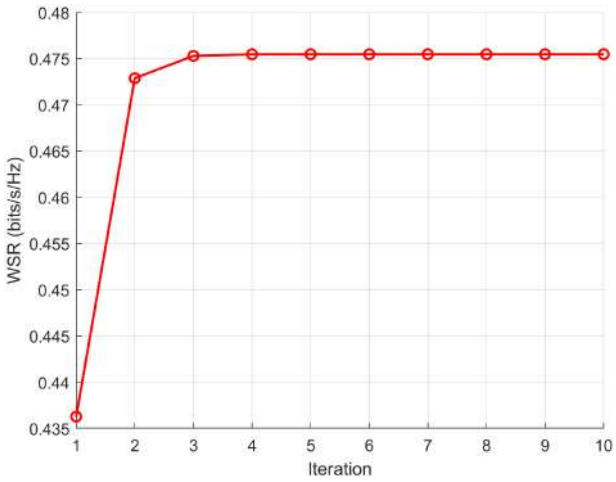

FIGURE 13. Convergence of alternating optimization algorithm for $K = 4$ at $P_{\max} = 20$ dBm.

1) STOCHASTIC SIMULATIONS

Revisiting Single-User Scenario: First, we set number of vehicles as $K = 1$ and evaluate the performance of the Algorithm 3. However, for this single user scenario there is no power control problem and also, MRC is optimal for receive filtering. Therefore, we fix the power at maximum power level and in addition, we use MRC in the alternating optimization algorithm presented in Section IV-C. The device positions are same as what we considered in Section V-A1.

The plot of achievable rates with transmit power is shown in Fig. 10. A significant increase in the achievable rate is observed while utilizing the RIS, validating the operation of alternating optimization algorithm that we developed. The performance of the algorithm is very close to the upper bound. As we can see, using random phase shifts at the RIS does not provide any improvement. However, random phase iteration provides somewhat higher performance compared to just setting phases randomly and for without RIS as well. Optimization problem for the single vehicle scenario is comparatively easier than multiple vehicle scenario. There is no interference and it is essentially a SNR maximization problem. Next, we will consider a multi-user scenario.

Multi-User Scenario: We consider a multi-user scenario with four vehicles. The positions of the vehicles, BS and RIS are shown in Fig. 11 with same heights as in Section V-A1. In order to provide fairness across all the users we set the weights of the users inversely proportional to the distant dependent path loss between the BS and the vehicle. We set the weight for the kth vehicle as

$$\tilde{u_k} = \frac{1}{L(d_k)} \tag{43a}$$

$$u_k = \frac{\tilde{u_k}}{\sum_{k=1}^{K} \tilde{u_k}}, \tag{43b}$$

where $L(d_k)$ denotes the distant dependent path loss and d_k is the distance between the BS and the kth vehicle.

Fig. 12 shows the plot of WSR with the variation of maximum transmit power. The results show that the RIS indeed provides a huge improvement to the WSR and results are quite close to the upper bound. EQP-MRC performs close to the results of Algorithm 3 at low transmit power levels, though the performance degradation increases as the transmit power is increased. In our system, interference is mitigated through both power allocation, and active and passive beamforming. For EQP-MRC, interference is mitigated only

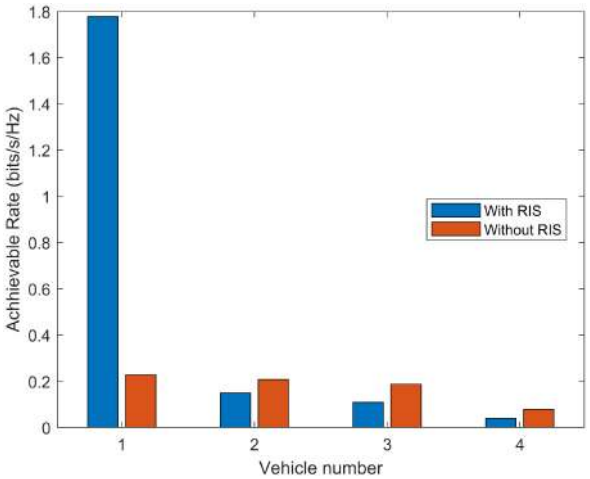

FIGURE 14. Per user achievable rates for $K = 4$ at $P_{max} = 20$ dBm.

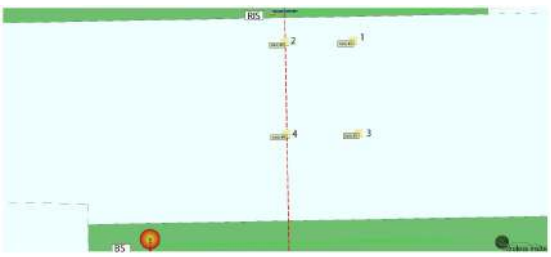

FIGURE 15. Simulating RIS aided multi vehicle system in Remcom Wireless InSite [28].

through phase optimization, which is sufficient when there is low interference. However, as the interference increases due to the increase of transmit power, receive beamforming and power allocation are also needed to obtain the required performance, which explains the superior performance of Algorithm 3. Fig. 13 shows the convergence of the alternating optimization algorithm for a certain channel realization. We can see that the algorithm converges quite fast, just under 3 iterations.

In both Fig. 10 and Fig. 12, we have included the results of position-based beamforming. We can see that, for the single user case, position-based beamforming performs close to full CSI results with only a small gap. However, for the multi-user case this performance gap is high. The reason for this is that, in multi-user case we need to consider LoS approximation for all the channels involved for each user. Each approximation introduces a certain error into beamforming algorithm, which adds up to less accurate beamforming for multi-user case. Still, it gives a considerable performance gain than the system without RIS.

Next, we look at per user rates to get a closer look at how the RIS has improved the communication. This is shown in Fig. 14 for a certain channel realization. We see that, without RIS all the users have low rates, and the rate of vehicle 1 has been significantly improved by utilizing the RIS. We note that, it is the vehicle closest to the RIS. However, the rates of other vehicles have been slightly reduced. Yet, the

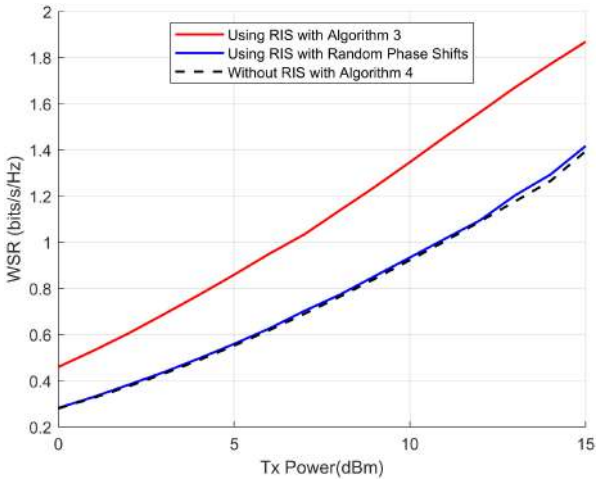

FIGURE 16. Variation of WSR with transmit power for $K = 4$ from the ray tracing based simulation.

RIS has enabled vehicle 1 to communicate with the BS at a high rate, even though it is not the closest vehicle to the BS. The communication link through RIS experiences high path loss due to the scattering nature of RIS elements. The benefits from passive beamforming get compromised by this high path loss, unless the user is in close vicinity.

These stochastic simulations carried so far have given us many useful insights into RIS aided vehicular communications. However, we based our simulations on a Rician fading model which relies on simplified assumptions. Therefore, we will next perform a realistic simulation using ray tracing to get practical insights.

2) RAY TRACING SIMULATIONS

We perform a ray tracing simulation using Wireless InSite [28] for multi-user scenario, similar to what we did for single user scenario. We model an urban scenario depicting buildings and roads, and consider four vehicles communicating with the BS. The BS is on the other side of the road away from the vehicles, and an RIS near the vehicles is used to assist the communication. The weights of the users are set using the weighting scheme (43b). Fig. 16 shows the plot of WSR with maximum transmit power. We see that the RIS provides a significant improvement in terms of the WSR.

Fig. 17 shows the per user rates for the ray tracing scenario. Vehicle 2 which is closest to the RIS has the lowest rate without RIS, but it has the highest rate with the help of RIS. The use of RIS has increased the rate of vehicle 2 remarkably. However, RIS does not provide any improvements to other vehicles. The reason for this is the double path loss experienced by the links through RIS as we saw earlier. Although passive beamforming can improve the communication significantly, the users need to be in close vicinity of the RIS in-order to get any benefits, similar to what we have seen in stochastic simulations.

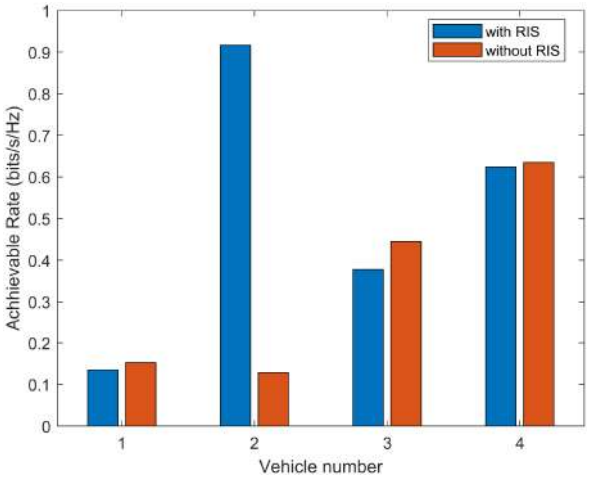

FIGURE 17. Per user achievable rates for $K = 4$ at $P_{\max} = 0$ dBm from the ray tracing based simulation.

TABLE 1. Maximum drop of channel magnitude.

Velocity	Maximum drop without RIS	Maximum drop with IRS
$5\ m/s$	21.7 dB	4.6 dB
$10\ m/s$	21.6 dB	4.7 dB
$20\ m/s$	23.1 dB	4.8 dB

C. MOBILITY SIMULATIONS

We have not considered mobility in our previous stochastic simulations. In our RIS aided system, the movement of the vehicle introduces a Doppler shift, or frequency shift, into the incident plane wave. The Doppler shift is given by

$$f_D = f_m \cos\theta \quad \text{Hz}, \tag{44}$$

where $f_m = \frac{v}{\lambda_c}$, v is the velocity of the vehicle, λ_c is the wavelength of the arriving plane wave and θ is the angle between direction of departure, and the moving direction of the vehicle. We modify the static Rician channel considered in (42) into a time varying channel. The time varying LoS component is given by

$$\boldsymbol{H}_{los}(t) = \sqrt{L_{los}} \exp(j2\pi f_D t) \exp\left(\frac{-j2\pi d}{\lambda}\right) \boldsymbol{a}_{rx} \boldsymbol{a}_{tx}^H, \tag{45}$$

where $\boldsymbol{a}_{rx}$ and $\boldsymbol{a}_{tx}^H$ are the array responses of receiver and transmitter. The time varying non-LoS component $\boldsymbol{H}_{nlos}(t)$ is generated by using a filtered white Gaussian noise (FWGN) model, independently for each receiver-transmitter pair. Based on this channel model, we perform several simulations to evaluate the mobility in the system. In these simulations, we solve the optimization problem at each point, using the algorithms developed.

Fig. 18(b) shows the variation of achievable rate as the vehicle moves along the given trajectory with a velocity of 10 m/s. Results show that, the achievable rate decreases exponentially as the vehicle moves away from the BS. The fading is more severe than the static case simulated with independent fading in each symbol, due to mobility. The RIS improves the achievable rate significantly when the vehicle is in close vicinity. However, in order to get a noticeable improvement, the vehicle needs to be in a certain range from the RIS, which is about 10 m as we see from the results.

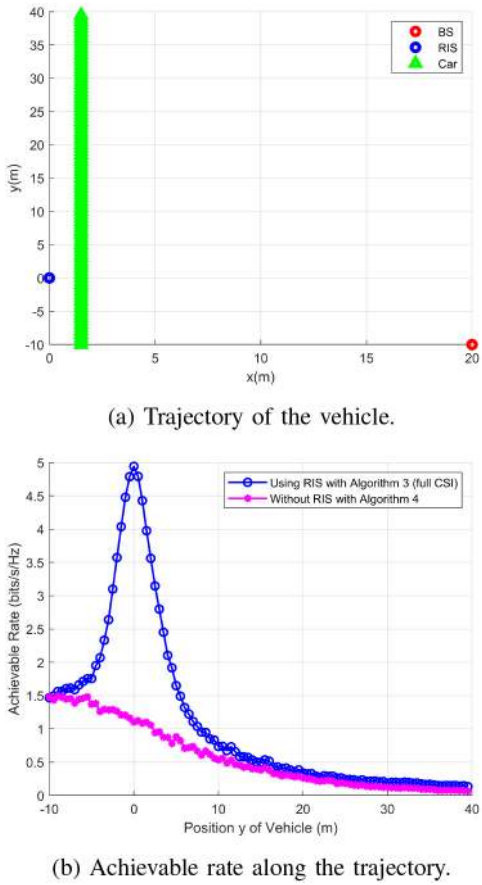

(a) Trajectory of the vehicle.

(b) Achievable rate along the trajectory.

FIGURE 18. Variation of achievable rate as the vehicle moves along a trajectory.

Then, we simulate the average achievable rate (AAR) when the vehicle is moving near the RIS as shown in Fig. 19(a), and the results are shown in Fig. 19(b). We can see that the AAR slightly decreases with the increasing velocity in the system without RIS. However, the RIS aided system shows a notably higher AAR compared to the system without RIS, and it stays stable across the considered velocities. In order to get a closer look at how the RIS improves the achievable rate of the vehicle, we can look at the channel magnitude. Fig. 20 shows the variation of channel magnitude in a certain period of time for the channel between the vehicle and a single antenna element of the BS, at different velocities of the vehicle. When looking at the direct link without RIS, we can see that the channel undergoes severe fading dips due to mobility. The frequency of these fading dips increases as the velocity increases, which explains the decrease in AAR with increasing velocity, as seen in Fig. 19(a). The maximum drop of channel magnitude for each case with and without RIS is given in TABLE 1. It shows that, the effective channel utilizing RIS has notably less severe dips compared to the direct channel, and it holds

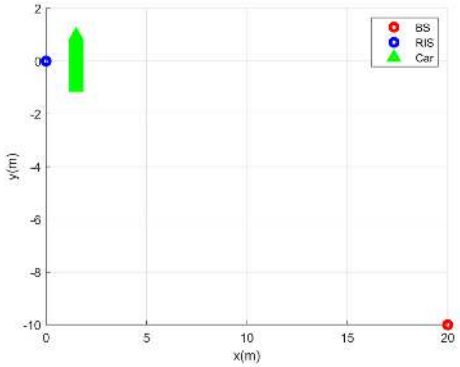

(a) Vehicle passing the RIS.

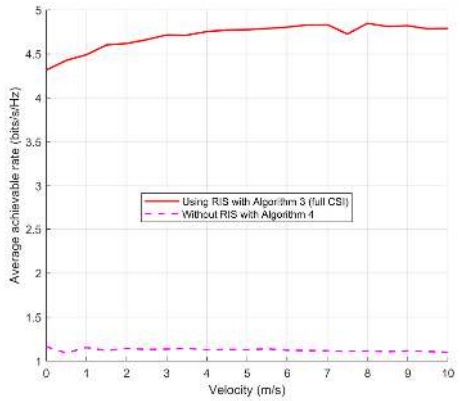

(b) Variation of average achievable rate with velocity of the vehicle.

FIGURE 19. Effect of velocity on the average achievable rate.

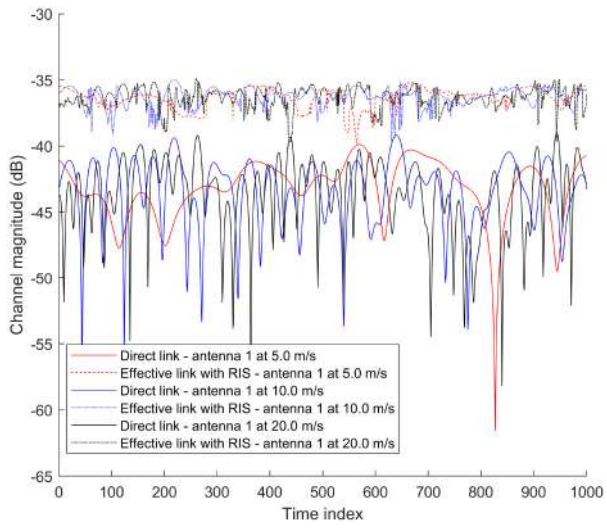

FIGURE 20. Variation of the magnitude of the channel with mobility.

this behavior across all the velocities that we have considered. For example, at 20 m/s the maximum drop in channel magnitude is about five times less while utilizing the RIS. These simulation results show the ability of the RIS to mitigate the effects of mobility, which enables its usage in a vehicular network.

VI. CONCLUSION

We have investigated an RIS aided mmWave vehicular communication system in this work. First, we have considered the achievable rate maximization in the uplink focusing on a single vehicle. We have developed a successive refinement based phase optimization algorithm, and we have proposed two passive-beamforming schemes that can be utilized to reduce the channel estimation overhead, which help enabling the practical usage of large reflecting arrays. Then, we have investigated multi-user communications, where we have considered the weighted sum rate maximization problem in the uplink. We have used fractional programming techniques to reformulate the problem into a more convenient form and developed an alternating optimization algorithm that solves the joint power control, receive filtering and phase optimization problem. The performance of the algorithms is verified through numerical simulations. The numerical results have shown that an RIS indeed provides a significant improvement to the communication system without RIS. Furthermore, we have used commercial ray tracing tool, Wireless Insite [28] to perform realistic ray tracing simulations. However, results have suggested that the vehicles need to be in close vicinity of the RIS to get significant benefits. Yet, RIS provides a way to enable communication at a high rate when the vehicle is close to RIS. The passive operation and low implementation cost make RIS a very appealing tool for future mmWave vehicular networks.

In our simulations we have studied the time varying channel of a moving vehicle. The results demonstrate the ability of the RIS to mitigate the effects of mobility to some extent, thus enabling its usage in a vehicular network. In the future, the current work will be extended to investigate the performance improvement of a high mobility user by associating more RISs to the network.

REFERENCES

[1] Q. Wu and R. Zhang, "Towards smart and reconfigurable environment: Intelligent reflecting surface aided wireless network," *IEEE Commun. Mag.*, vol. 58, no. 1, pp. 106–112, Jan. 2020.

[2] E. Björnson, Ö. Özdogan, and E. G. Larsson, "Reconfigurable intelligent surfaces: Three myths and two critical questions," *IEEE Commun. Mag.*, vol. 58, no. 12, pp. 90–96, Dec. 2020.

[3] Q. Wu, S. Zhang, B. Zheng, C. You, and R. Zhang, "Intelligent reflecting surface aided wireless communications: A tutorial," *IEEE Trans. Commun.*, early access, Jan. 18, 2021, doi: 10.1109/TCOMM.2021.3051897.

[4] S. Hu, F. Rusek, and O. Edfors, "The potential of using large antenna arrays on intelligent surfaces," in *Proc. IEEE 85th Veh. Technol. Conf. (VTC Spring)*, 2017, pp. 1–6.

[5] Q. Wu and R. Zhang, "Intelligent reflecting surface enhanced wireless network via joint active and passive beamforming," *IEEE Trans. Wireless Commun.*, vol. 18, no. 11, pp. 5394–5409, Nov. 2019.

[6] Q. Wu and R. Zhang, "Beamforming optimization for wireless network aided by intelligent reflecting surface with discrete phase shifts," *IEEE Trans. Commun.*, vol. 68, no. 3, pp. 1838–1851, Mar. 2020.

[7] E. Basar, I. Yildirim, and I. F. Akyildiz, "Indoor and outdoor physical channel modeling and efficient positioning for reconfigurable intelligent surfaces in mmWave bands," 2020. [Online]. Available: arXiv:2006.02240.

[8] E. Basar and I. Yildirim, "SimRIS channel simulator for reconfigurable intelligent surface-empowered communication systems," in *Proc. IEEE Lat. Amer. Conf. Commun. (LATINCOM)*, 2020, pp. 1–6.

[9] Y. Yang, B. Zheng, S. Zhang, and R. Zhang, "Intelligent reflecting surface meets OFDM: Protocol design and rate maximization," *IEEE Trans. Commun.*, vol. 68, no. 7, pp. 4522–4535, Jul. 2020.

[10] K. Ying, Z. Gao, S. Lyu, Y. Wu, H. Wang, and M. Alouini, "GMD-based hybrid beamforming for large reconfigurable intelligent surface assisted millimeter-wave massive MIMO," *IEEE Access*, vol. 8, pp. 19530–19539, 2020.

[11] A. Taha, M. Alrabeiah, and A. Alkhateeb, "Enabling large intelligent surfaces with compressive sensing and deep learning," 2019. [Online]. Available: arXiv:1904.10136.

[12] G. Zhou, C. Pan, H. Ren, K. Wang, M. D. Renzo, and A. Nallanathan, "Robust beamforming design for intelligent reflecting surface aided MISO communication systems," *IEEE Wireless Commun. Lett.*, vol. 9, no. 10, pp. 1658–1662, Oct. 2020.

[13] G. Zhou, C. Pan, H. Ren, K. Wang, and A. Nallanathan, "A framework of robust transmission design for IRS-aided MISO communications with imperfect cascaded channels," *IEEE Trans. Signal Process.*, vol. 68, pp. 5092–5106, Aug. 2020, doi: 10.1109/TSP.2020.3019666.

[14] F. Jameel, S. Wyne, S. J. Nawaz, and Z. Chang, "Propagation channels for mmWave vehicular communications: State-of-the-art and future research directions," *IEEE Wireless Commun.*, vol. 26, no. 1, pp. 144–150, Feb. 2019.

[15] N. Jayaweera, N. Rajatheva, and M. Latva-Aho, "Autonomous driving without a burden: View from outside with elevated LiDAR," in *Proc. IEEE 89th Veh. Technol. Conf. (VTC-Spring)*, 2019, pp. 1–7.

[16] Z. Sheng, A. Pressas, V. Ocheri, F. Ali, R. Rudd, and M. Nekovee, "Intelligent 5G vehicular networks: An integration of DSRC and mmWave communications," in *Proc. Int. Conf. Inf. Commun. Technol. Convergence (ICTC)*, 2018, pp. 571–576.

[17] P. Nelson. (Dec. 2016). *Just One Autonomous Car Will Use 4,000 GB of Data/Day*. [Online]. Available: https://www.networkworld.com/article/3147892/one-autonomous-car-will-use-4000-gb-of-dataday.html

[18] A. Alkhateeb, J. Mo, N. Gonzalez-Prelcic, and R. W. Heath, "MIMO precoding and combining solutions for millimeter-wave systems," *IEEE Commun. Mag.*, vol. 52, no. 12, pp. 122–131, Dec. 2014.

[19] P. Wang, J. Fang, X. Yuan, Z. Chen, H. Duan, and H. Li, "Intelligent reflecting surface-assisted millimeter wave communications: Joint active and passive precoding design," 2019. [Online]. Available: arXiv:1908.10734.

[20] A. Makarf *et al.*, "Reconfigurable intelligent surfaces-enabled vehicular networks: A physical layer security perspective," 2020. [Online]. Available: arXiv:2004.11288.

[21] J. Wang, W. H. Zhang, X. Bao, T. Song, and C. Pan, "Outage analysis for intelligent reflecting surface assisted vehicular communication networks," 2020. [Online]. Available: arXiv:2004.08063.

[22] Y. Chen, Y. Wang, J. Zhang, and Z. Li, "Resource allocation for intelligent reflecting surface aided vehicular communications," *IEEE Trans. Veh. Technol.*, vol. 69, no. 10, pp. 12321–12326, Oct. 2020.

[23] C. Pan *et al.*, "Multicell MIMO communications relying on intelligent reflecting surfaces," *IEEE Trans. Wireless Commun.*, vol. 19, no. 8, pp. 5218–5233, Aug. 2020.

[24] Z. Zhang and L. Dai, "Capacity improvement in wideband reconfigurable intelligent surface-aided cell-free network," in *Proc. IEEE 21st Int. Workshop Signal Process. Adv. Wireless Commun. (SPAWC)*, 2020, pp. 1–5.

[25] H. Guo, Y.-C. Liang, J. Chen, and E. G. Larsson, "Weighted sum-rate maximization for reconfigurable intelligent surface aided wireless networks," *IEEE Trans. Wireless Commun.*, vol. 19, no. 5, pp. 3064–3076, May 2020.

[26] K. Shen and W. Yu, "Fractional programming for communication systems—Part II: Uplink scheduling via matching," *IEEE Trans. Signal Process.*, vol. 66, no. 10, pp. 2631–2644, May 2018.

[27] D. Dampahalage, K. B. S. Manosha, N. Rajatheva, and M. Latva-Aho, "Intelligent reflecting surface aided vehicular communications," in *Proc. IEEE Globecom Workshops (GC Wkshps)*, 2020, pp. 1–6.

[28] Remcom, Inc. (2020). *Wireless InSite*. [Online]. Available: http://www.remcom.com/wireless-insite

[29] Y. Zhao, Y. Liu, G. Boudreau, A. B. Sediq, and X. Wang, "Angle-based beamforming in mmWave massive MIMO systems with low feedback overhead using multi-pattern codebooks," *China Commun.*, vol. 16, no. 9, pp. 18–30, 2019.

[30] T. Shimizu, V. Va, G. Bansal, and R. W. Heath, "Millimeter wave V2X communications: Use cases and design considerations of beam management," in *Proc. Asia Pac. Microw. Conf. (APMC)*, 2018, pp. 183–185.

[31] S. Boyd and L. Vandenberghe, *Convex Optimization*, Cambridge, U.K.: Cambridge Univ. Press, 2004.

[32] "Study on channel model for frequencies from 0.5 to 100 GHz, v16.1.0," 3GPP, Sophia Antipolis, France, Rep. TR 38.901, Dec. 2019.

[33] B. Colo, A. Fouda, and A. S. Ibrahim, "Ray tracing simulations in millimeter-wave vehicular communications," in *Proc. IEEE 30th Annu. Int. Symp. Pers. Indoor Mobile Radio Commun. (PIMRC)*, 2019, pp. 1–4.

DILIN LALINDRA DAMPAHALAGE (Graduate Student Member, IEEE) received B.Sc. (Hons.) degree in electronics and telecommunication engineering from the University of Moratuwa, Sri Lanka, in 2018, and the M.Sc. (Technology) degree in wireless communications engineering from the University of Oulu, Finland, in 2020, where he is currently pursuing the Ph.D. degree with the Centre for Wireless Communications. His research interests include reconfigurable intelligent surfaces, vehicular communications and application of optimization techniques for wireless communications.

K. B. SHASHIKA MANOSHA (Member, IEEE) received the B.Sc. (Eng.) degree in electrical and information engineering from the University of Ruhuna, Matara, Sri Lanka, the M.Eng. degree in information and communication technologies from the Asian Institute of Technology, Thailand, and the Dr.Sc. (Tech.) degree in telecommunications engineering from the University of Oulu, Finland, where he has worked as a Postdoctoral Researcher with the Center for Wireless Communication for a year. Then he joined Keysight Technologies, Oulu, Finland, as a Research and Development Engineer with the Channel Modeling and Solutions Team. At Keysight, he worked for two years contributing to OTA chamber development and providing channel models for equipment testing. He is currently working as a Senior Research Specialist with the S&R Lab, Nokia Networks and Solutions Oy, Oulu, Finland. His research interests include massive MIMO communications, wireless channel modeling and OTA, L1 and L2 signaling, and application of optimization techniques for wireless communications.

NANDANA RAJATHEVA (Senior Member, IEEE) received the B.Sc. (Hons.) degree in electronics and telecommunication engineering from the University of Moratuwa, Sri Lanka, in 1987, ranking first in the graduating class, and the M.Sc. and Ph.D. degrees from the University of Manitoba, Winnipeg, MB, Canada, in 1991 and 1995, respectively. He is currently a Professor with the Centre for Wireless Communications, University of Oulu, Finland. He was a Canadian Commonwealth Scholar during the graduate studies in Manitoba. He held a Professor/Associate Professor positions with the University of Moratuwa and the Asian Institute of Technology, Thailand, from 1995 to 2010. He is currently leading the AI-driven Air Interface design task in Hexa-X EU Project. He has coauthored more than 200 refereed papers published in journals and in conference proceedings. His research interests include physical layer in beyond 5G, machine learning for PHY and MAC, sensing for factory automation and channel coding.

MATTI LATVA-AHO (Senior Member, IEEE) received the M.Sc., Lic.Tech., and Dr.Tech. (Hons.) degrees in electrical engineering from the University of Oulu, Finland, in 1992, 1996, and 1998, respectively. From 1992 to 1993, he was a Research Engineer with Nokia Mobile Phones, Oulu, Finland, after which he joined the Centre for Wireless Communications (CWC). He was the Director of CWC from 1998 to 2006, and the Head of the Department for Communication Engineering until August 2014. He currently serves as an Academy of Finland Professor and the Director for National 6G Flagship Programme. He has published close to 500 conference or journal papers in the field of wireless communications. His research interests are related to mobile broadband communication systems and his group currently focuses on beyond 5G systems research. He received the Nokia Foundation Award in 2015 for his achievements in mobile communications research.